Large-Scale Impact of CO_2 Storage in Deep Saline Aquifers: A Sensitivity Study on Pressure Response in Stratified Systems

Jens T. Birkholzer *, Quanlin Zhou, and Chin-Fu Tsang

Earth Sciences Division, Lawrence Berkeley National Laboratory, University of California, Berkeley, CA 94720, USA

Abstract

Large volumes of CO_2 captured from carbon emitters (such as coal-fired power plants) may be stored in deep saline aquifers as a means of mitigating climate change. Storing these additional fluids may cause pressure changes and displacement of native brines, affecting subsurface volumes that can be significantly larger than the CO_2 plume itself. This study aimed at determining the three-dimensional region of influence during/after injection of CO_2 and evaluating the possible implications for shallow groundwater resources, with particular focus on the effects of interlayer communication through low-permeability seals. To address these issues quantitatively, we conducted numerical simulations that provide a basic understanding of the large-scale flow and pressure conditions in response to industrial-scale CO_2 injection into a laterally open saline aquifer. The model domain included an idealized multilayered groundwater system, with a sequence of aquifers and aquitards (sealing units) extending from the deep saline storage formation to the uppermost freshwater aquifer. Both the local CO_2-brine flow around the single injection site and the single-phase water flow (with salinity changes) in the region away from the CO_2 plume were simulated. Our simulation results indicate considerable pressure buildup in the storage formation more than 100 km away from the injection zone, whereas the lateral distance migration of brine is rather small. In the vertical direction, the pressure perturbation from CO_2 storage may reach shallow groundwater resources only if the deep storage formation communicates with the shallow aquifers through sealing units of relatively high permeabilities (higher than 10×18 m^2). Vertical brine migration through a sequence of layers into shallow groundwater bodies is extremely unlikely. Overall, large-scale pressure changes appear to be of more concern to groundwater resources than changes in water quality caused by the migration of displaced saline water.

Keywords: geological sequestration, saline aquifer, pressure buildup, numerical simulation, multilayered system

1. Introduction

Geologic carbon sequestration in deep formations (e.g., saline aquifers, oil and gas reservoirs, and coalbeds) has drawn increasing consideration as a promising method to mitigate the adverse impacts of climate change (Holloway, 1996; Gale, 2004; IPCC, 2005; Hepple and Benson, 2005). Deep saline aquifers offer the largest storage potential of all the geological CO_2 storage options and are widely distributed throughout the globe in all sedimentary basins. ForCO_2 storage to have a significant impact on atmospheric levels of greenhouse gases, the amounts of CO_2 injected and sequestered underground need to be extremely large (Holloway, 2005). Various research studies have been conducted to date evaluating under which hydrogeological

conditions the injected volumes of CO_2 can be safely stored over hundreds or even thousands of years. For example, many of these studies address issues such as the long-term efficiency of structural trapping of CO_2 under sealing layers. Less emphasis has been placed on evaluating the large-scale pressure changes caused by industrial-scale injection of CO_2 into deep saline formations or understanding the fate of the native brines that are being displaced by the injected fluids (Van der Meer, 1992; Holloway, 1996; Gunter et al., 1996). Large-scale injection of CO_2 will impact subsurface volumes much larger than the CO_2 plume. Thus, even if the injected CO_2 itself is safely trapped in suitable geological structures, pressure changes and brine displacement may affect shallow groundwater resources, for example, by increasing the rate of discharge into a lake or stream, or by mixing of brine into drinking water aquifers (Bergman and Winter, 1995).

Fig. 1 shows schematically the large-scale subsurface impacts that may be experienced during and after industrial-scale injection of CO_2. While the CO_2 plume at depth may be safely trapped under a low-permeability caprock with an anticlinal structure, the footprint area of the plume is much smaller than the footprint area of elevated pressure expected in the storage formation. The environmental impact of large-scale pressure buildup and related brine displacement depends mainly on the hydraulic connectivity between deep saline formations and the freshwater aquifers overlying them. One concern would be a storage formation that extends updip to form a freshwater resource used for domestic or commercial water supply (Bergman and Winter, 1995; Nicot, 2008). Via this direct hydraulic communication, CO_2 storage at depth could impact the shallow portions of the aquifer, which may experience water table rise, changes in discharge and recharge zones, and changes in water quality. Even if separated from deep storage formations by low-permeability seals, freshwater resources may be hydraulically communicating with deeper layers, and the pressure buildup at depth would then provide a driving force for upward brine migration. Interlayer pressure propagation and brine leakage may occur, for example, if high-permeability conduits such as faults and abandoned boreholes are present. Pressure may also propagate in a slow, diffuse process if the sealing layers have a relatively high permeability.

A recent study of CO_2 storage capacity in compartmentalized saline formations suggests that the hydraulic characteristics of seal layers may strongly affect the lateral and vertical volumes affected by pressure buildup (Zhou et al., 2008). Suitable sites for CO_2 sequestration would typically have thick, laterally continuous shale, mudstone, or siltstone seals that act as permeability and capillary barriers to impede or prevent upward migration of buoyant CO_2. These sealing units also play a role in reducing the interlayer pressure perturbation and limiting flow of native brine out of the storage formation into overlying and underlying strata. In contrast to supercritical CO_2, however, this process is limited only by the small seal permeability; capillary sealing is not a factor. Interlayer pressure propagation and brine leakage may occur anywhere in the storage formation where pressure increases in response to CO_2 injection. Thus, these processes can occur over a large area.

How far the pressure buildup induced by CO_2 injection will extend into the lateral versus the vertical direction depends on the characteristics and properties of the stratigraphic units. If brine leakage out of the storage formation were important, the lateral displacement of brine within the formation would become less extensive, and vice versa. For very small seal permeabilities, the native brine displaced by injected CO_2 is expected to migrate mostly within the storage formation, which could potentially affect freshwater resources located further updip (Fig. 1) (Nicot, 2008). On the other hand, if the

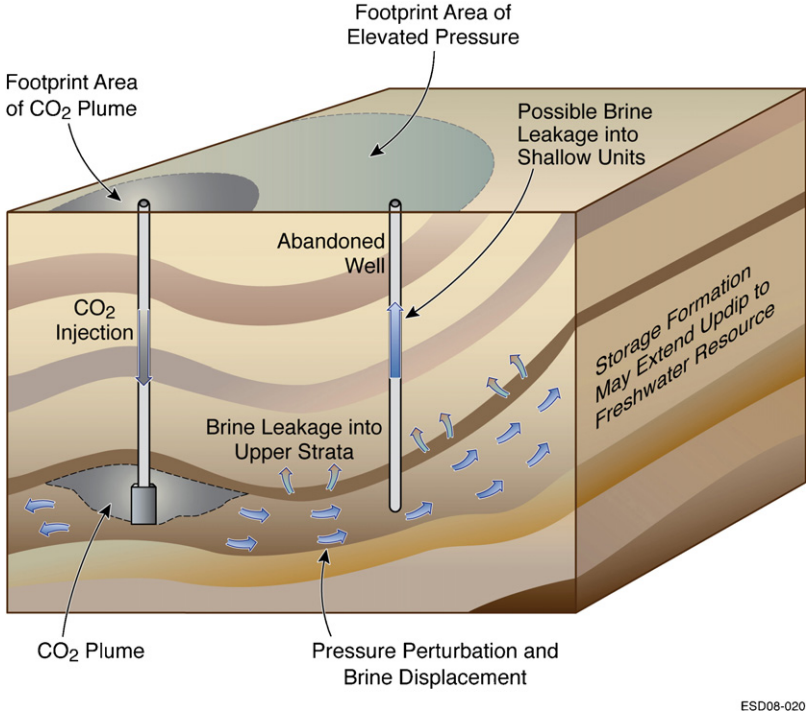

Fig. 1 – Schematic showing different regions of influence related to CO_2 storage.

sealing layers have a relatively higher permeability, the pressure front (and the native brine) may slowly propagate into and through the seals into neighboring formations, and may reach shallow levels in extreme cases. At the same time, such considerable vertical leakage would attenuate pressure buildup within the storage formation.

To our knowledge, no research has been conducted to date to systematically estimate the area of influence in response to CO_2 storage within multilayer systems where lateral and vertical brine flow may compete. This article describes an attempt to address these issues quantitatively, providing a basis for further studies directly addressing the potential environmental risks to groundwater resources. Numerical simulations are conducted to estimate the pressure perturbation and brine migration in response to industrial-scale CO_2 injection into a large, laterally open saline aquifer. The model domain includes an idealized multilayer groundwater system, with a sequence of aquifers and aquitards (sealing layers) extending from the deep saline storage formation to the top of the uppermost freshwater aquifer. Thereby, the region of influence is evaluated in both lateral and vertical directions. Recognizing the possible importance of vertical interlayer communication, we conduct sensitivity studies, varying the hydrologic properties of the aquitards. Our research aims at: (1) developing a basic understanding of flow and pressure conditions in a CO_2 storage formation embedded in a sequence of aquifers and aquitards, (2) exploring the effects of interlayer communication through low-permeability seals and the impact on lateral/vertical displacement, and (3) determining the region of influence during/after injection of CO_2 and evaluating possible implications for shallow groundwater resources.

2. Model setup and parameters

A numerical model is developed to investigate the multiphase flow and multicomponent transport of CO_2 and brine in response to CO_2 injection into an idealized multilayer formation. The transient pressure buildup, spatial CO_2 plume evolution, and brine flow and transport are simulated for various sensitivity cases, using the TOUGH2/ECO2N simulator (Pruess et al., 1999; Pruess, 2005).

2.1. *Conceptual model and model setup*

A two-dimensional radially symmetric model domain was chosen to represent a CO_2 storage site with a deep saline aquifer underlying a typical aquifer/aquitard (e.g., sandstone/shale) stratigraphy. The storage formation into which CO_2 is injected is 60 m thick and located at a depth of about 1200 m (bottom of formation) below the ground surface. The storage formation is bounded at the top by a sealing layer 100 m thick, followed by a sequence of 60 m thick aquifers and 100 m thick sealing layers (see Fig. 2). The bottom of the storage formation is formed by impermeable base rock. Altogether, the model domain includes eight aquifers and seven aquitards, with Aquifer 1 the storage formation, Aquitard 1 the primary sealing unit above the storage formation, and Aquifer 8 the uppermost aquifer nearest to the ground surface, assumed to be confined in this study. The lateral extent of the model domain is set to R = 200 km, which corresponds to a footprint area of more than 125,000 km^2; this large lateral extent was chosen to ensure that the boundary condition would have minimal effect on the simulation results. The lateral boundary at 200 km, where the initial hydrostatic pressure is specified, is open for fluids to escape from the model domain.

Carbon dioxide is injected into a zone of 50 m radial extent, representing not a single well, but rather a few distributed wells. Injection occurs over 30 years at an annual rate of 1.52 million tonnes of CO_2, representing the CO_2 rate captured from a medium-size coal-fired power plant. The simulation runs cover a time period of 100 years altogether, comprising the 30-year injection period and a 70-year post-injection period. As CO_2 is injected, the additional fluid is initially accommodated by

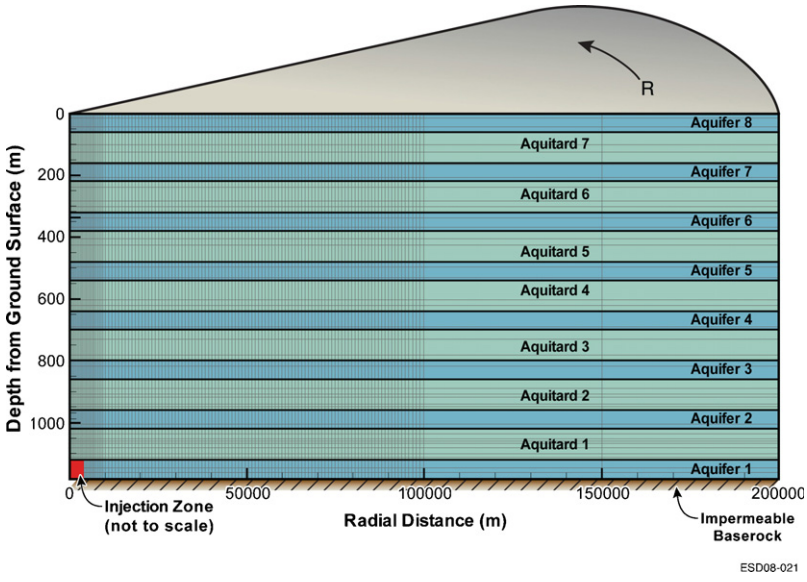

Fig. 2 – Schematic showing a vertical cross-section of the radially symmetric model domain with a deep brine formation for CO_2 storage and overlying aquifer/aquitard sequence. The numerical simulation grid is also depicted.

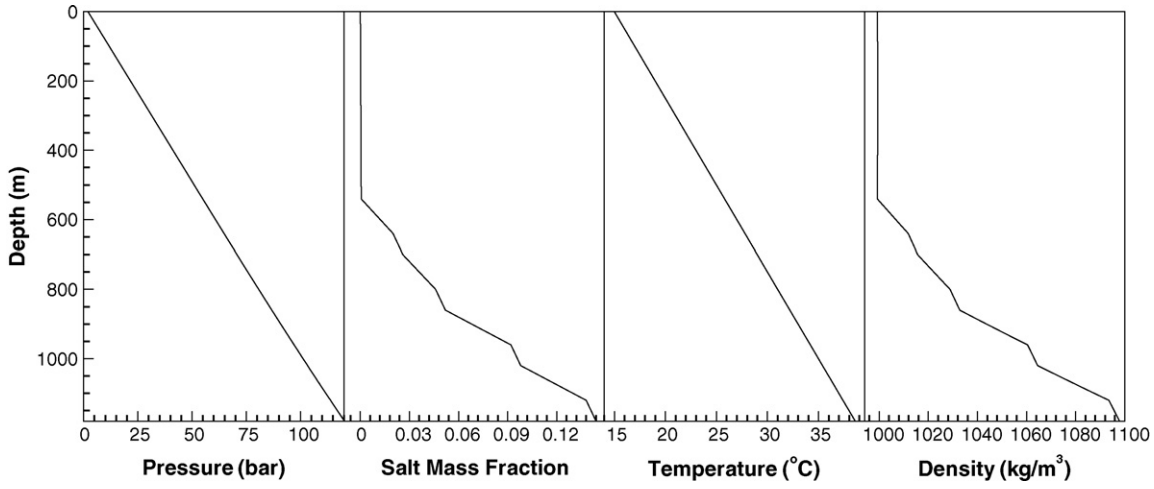

Fig. 3 – Vertical profiles of initial pressure, salt mass fraction, temperature, and brine density from the top aquifer near the ground surface to the storage formation.

localized pressure buildup, causing pore expansion and fluid density increases, and by phase volume reduction resulting from dissolution of supercritical CO_2 into the aqueous phase. After injection stops, the pressure-perturbed system will tend to relax and return to an equilibration state, generally long after injection ceases. While pore (or matrix) compressibility and fluid density changes (CO_2 and brine) are accounted for in the TOUGH2/ECO2N multiphase simulations, geomechanical effects such as land-surface uplift are not explicitly considered. These may change surface and near-subsurface flow patterns even without direct hydraulic impact. The reverse effect, land subsidence in response to groundwater withdrawal (e.g., for water supply, agriculture, or related to oil production), is a common problem throughout the United States (USGS, 1999). Furthermore, while the TOUGH2/ECO2N simulator considers CO_2 dissolution, other geochemical processes, such as CO_2 precipitation as carbonate minerals – a slow process leading to trapping of CO_2 in solid phase – are neglected.

Fig. 3 shows the initial conditions used for the simulations in a vertical profile. There is no lateral variation; i.e., the system is stagnant prior to injection of CO_2, meaning that regional groundwater flow is neglected. Initial pressure is hydrostatic. Temperature varies linearly with depth from 15 °C at the top to 38.6 °C at the bottom, assuming a geothermal gradient of 2 °C per 100 m depth. Low salinity levels (less than 500 mg/L) representative of fresh water are assumed over the top 540 m of the model domain, followed by increasing salinity levels with depth. In other words, in this scenario, the top four aquifers, referred to as Aquifers 5 through 8, are considered freshwater resources that would need to be protected. The maximum mass fraction of salt in brine in the CO_2 storage formation is 0.144, which compares to a salinity of approximately 156,000 mg/L. The vertical salinity profile represents an equilibrated system where no density-driven flow occurs at the initial state.

Notice that the simulation study does not consider direct high-permeability conduits between the deep saline formation and the shallow aquifers. The environmental concerns resulting from brine leakage via faults and abandoned boreholes will be addressed in future analyses.

2.2. *Model parameters*

The hydrogeologic properties chosen for the aquifer–aquitard sequence are given in Table 1. For simplification, in most simulation cases, all aquifers and all aquitards have been assigned the same set of aquifer and aquitard properties, respectively, without variation in depth. The (homogeneous) properties of the aquifers are typical of sedimentary formations suitable for CO_2 storage, with high-enough permeability and porosity. The (homogeneous) properties of all sealing layers are representative of shale formations suitable for trapping CO_2, with small permeability and high capillary entry pressure for supercritical CO_2. With the focus on the multilayer impact of

Table 1 – Hydrogeologic properties for the aquifer–aquitard system used in the simulations

Properties	Values for aquifers	Values for aquitards
Permeability, k (m^2)	1.0×10^{-13}	1.0×10^{-16} to 1.0×10^{-21}, and 0
Pore compressibility, β_p (Pa^{-1})	4.5×10^{-10}	9.0×10^{-10}
Porosity, ϕ	0.20	0.05
van Genuchten m	0.46	0.46
van Genuchten α (Pa^{-1})	5.0×10^{-5}	5.0×10^{-7}
Residual CO_2 saturation	0.25	0.35
Residual water saturation	0.30	0.30

CO_2 injection, which depends strongly on the properties of the sealing layers, we have varied seal permeability over a wide range: $k_s = 1.0 \times 10^{-16}$ to 1.0×10^{-21} m^2 – based on shale permeabilities reported in Neuzil (1994), Domenico and Schwartz (1998), Hovorka et al. (2001), and Hart et al. (2006) – plus one case with an impermeable seal for comparison. Notice that the van Genuchten model was used to calculate the capillary pressure and relative permeability of the two-phase flow in all simulation cases (Van Genuchten, 1980). This model contains two fitting parameters α and m; the van Genuchten α parameter represents roughly the inverse of the capillary entry pressure for the nonwetting phase, and the van Genuchten m parameter is a measure of the pore-size distribution.

Further simulation cases address sensitivity to pore compressibility, which is another key parameter defining the pressure response to CO_2 injection. In the first sensitivity case, the compressibility of all layers is considered to vary linearly with depth, starting with the values given in Table 1 for the deepest aquifer and aquitard, respectively, and assuming a one-order-of-magnitude increase over the entire vertical sequence (to account for the fact that shallower units are often less consolidated and thus more compressible than deep units). In two other sensitivity cases, we have reduced/increased the base-case compressibility values by one order of magnitude. The different cases reflect the range of pore compressibilities measured over a wide range of subsurface materials (e.g., Fjaer et al., 1991; Domenico and Schwartz, 1998; Hart, 2000; Harris, 2006). Note that the compressibility of the fluids (i.e., CO_2 and water) is intrinsically taken into account in TOUGH2/ECO2N in terms of density variations with fluid pressure. The sensitivity cases addressing pore compressibility have all been conducted using a seal permeability of 10^{-18} m^2, a value representative of the caprock of the Sleipner site, Norway, and the Frio site, Texas, USA (Hovorka et al., 2001; Chadwick et al., 2007).

3. Simulation results and discussion

3.1. *Spatial distribution of CO_2 plume*

Before elaborating on the large-scale impacts of CO_2 injection, we may briefly focus on the characteristics of the CO_2 plume at the end of the injection period, shown in Fig. 4, together with pressure buildup contours and brine flow vectors. The case depicted in the figure has a seal permeability of 10^{-18} m^2; all other properties are given in Table 1. Only a small part of the entire model domain is shown, concentrating on the storage formation near the injection point.

The CO_2 plume size is illustrated in Fig. 4 using saturation contours for supercritical CO_2. The plume is a little more than 2 km wide and is concentrated at the top of the storage formation, a result of buoyancy forces. In response to storage of additional fluid volumes, the fluid pressure in the storage formation has built up to maximum values above 50 bar near the injection zone. According to current practice for underground injection control of liquid wastes, the maximum injection pressure needs to be less than the measured *fracture closure pressure* in order to avoid geomechanical damage (USEPA, 1994). The regional guidance for implementation is that the maximum injection pressures can be determined either by a site-specific fracture closure pressure derived from direct or indirect testing, or by formation-specific default values for the fracture-closure pressure gradients. For example, 0.181 bar/m (i.e., ≈80% increase above the hydrostatic pressure gradient) is reported for the Dundee Limestone in the Michigan Basin in USA. In comparison, the pressure increase of 50 bar observed in the simulation example corresponds to 40% of the hydrostatic pressure gradient.

The region of significant pressure increases extends far in the lateral direction much further than the limited extent of the CO_2 plume. Though the characteristics of the sealing layer above the storage formation provide a safe structural trap for the CO_2 plume (owing to the combined effect of permeability and capillary barriers), the seal permeability is high enough to allow for pressure changes throughout the sealing layer and into upper strata. In fact, small pressure perturbation can be observed in the two deep aquifers immediately above the storage formation (Aquifers 2 and 3). The local pressure decrease in the sealing layer immediately above the CO_2 plume is a result of two-phase flow effects, which tend to reduce the amount of brine displaced from the storage formation into the upper units.

The water flux vectors in Fig. 4 indicate horizontal brine flow within the storage formation, with the exception of the plume area where buoyant CO_2 migration generates a down-

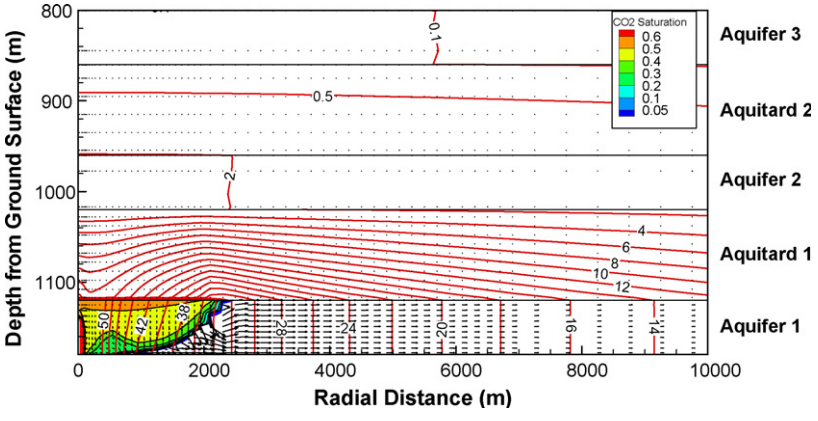

Fig. 4 – Contours of CO_2 saturation (flooded contours) and pressure buildup, given in bar (lines), as well as water flux vectors in m/s at the end of the injection period (30 years), obtained for the base case with a seal permeability of 10^{-18} m^2.

ward component of brine flow. The vector length corresponds to the magnitude of water flux, with the result that the low-velocity flow in the seals is too small to be visible. Notice that the CO_2 plumes are basically identical for all seal permeability cases, with the exception of the case of 10^{-16} m^2 permeability (these cases are not shown here for brevity). In this case, a minor fraction of the plume migrates into the sealing unit immediately above the storage formation (Aquifer 1) after 30 years of injection, indicating that CO_2 may not be safely trapped over longer time periods.

3.2. *Lateral and vertical pressure buildup*

In this section, we evaluate the large-scale pressure perturbations in the subsurface in response to CO_2 injection. Figs. 5 and 6 show contours of pressure buildup in a vertical cross-section that expands from the injection zone up to a lateral radius of 100 km and includes the entire vertical sequence of strata, from the deep storage formation all the way to the uppermost freshwater aquifer. Results are given at the end of the 30-year injection period and at 100 years after the onset of injection, respectively. Four simulation cases are considered, the differences among them being that the aquitards have permeabilities of $k_s = 10^{-17}$, 10^{-18}, 10^{-19}, and 10^{-20} m^2 (corresponding to a hydraulic conductivities ranging from 0.01 to 0.00001 millidarcy). A cutoff value of 0.1 bar is set for the contours; in other words, pressure buildup less than 0.1 bar, or less than a 1 m increase in groundwater elevation, is not colored.

It is obvious from Figs. 5 and 6 that the permeability of the sealing layers has a strong effect on both the vertical and the lateral pressure propagation. At the end of the injection period (Fig. 5), the low-permeability case (10^{-20} m^2) shows a pressure increase of 0.1 bar extending almost 85 km laterally within the storage formation, corresponding to an area of influence covering more than 22,000 km^2. This large area compares to the CO_2 plume of a little more than 2 km radial extent (Fig. 4). A 2-bar pressure buildup, equal to a 20 m increase in piezometric head, is observed at 45 km radial extent. Instead of the horizontal stratigraphy used in our simulations, we may imagine a gently updipping formation that forms a confined freshwater aquifer at 45 km distance. Ignoring the impact of vertical variations in salinity and compressibility, the shallow groundwater resource would then experience a piezometric head change of about 20 m. In the vertical direction, the region of pressure buildup is safely constrained to the lower portion of the sealing unit immediately above the storage formation.

With increasing seal permeability, a different behavior occurs. The high-permeability case (10^{-17} m^2), for example, has a lateral area of pressure increase extending to less than 50 km in the radial direction, covering about 7500 km^2. Also, the maximum pressure near the injection zone is reduced compared to the cases with smaller seal permeability. There is, on the other hand, significant pressure propagation upward from the storage formation, as apparent from pressure increases extending all the way to a depth of about 300 m from the ground surface—affecting Aquifers 5 and 6, which are considered freshwater resources. Intermediate results are obtained in the other two cases, with the case of 10^{-18} m^2 allowing pressure buildup up to a depth of 800 m, affecting the deepest three saline aquifers (Aquifers 1, 2, and 3). Clearly, in cases with comparably high seal permeability, brine leakage resulting from interlayer communication has a positive attenuation effect on the pressure conditions *within* the storage formation, while allowing for *vertical* pressure propagation that may possibly reach shallow aquifers. While

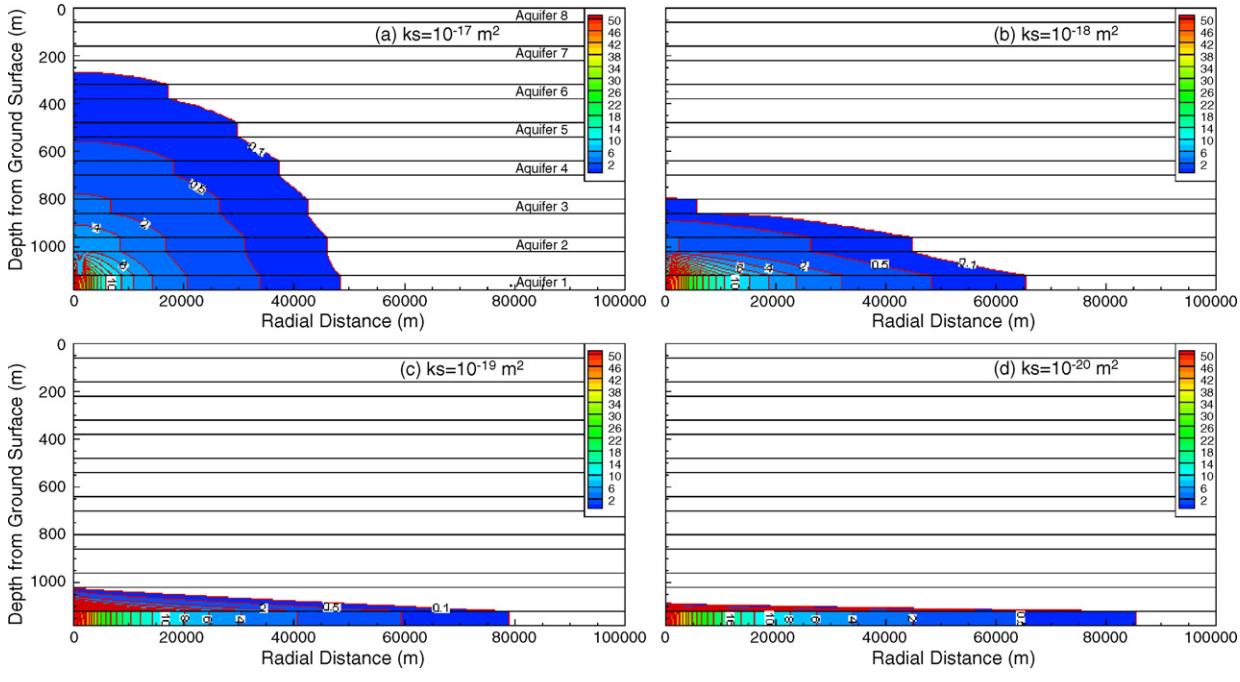

Fig. 5 – Contours of pressure buildup, given in bar (change in fluid pressure from the initial hydrostatic condition), at 30 years of CO_2 injection, for different values of seal permeability. A cutoff value of 0.1 bar is set for the contours. k_s means seal permeability.

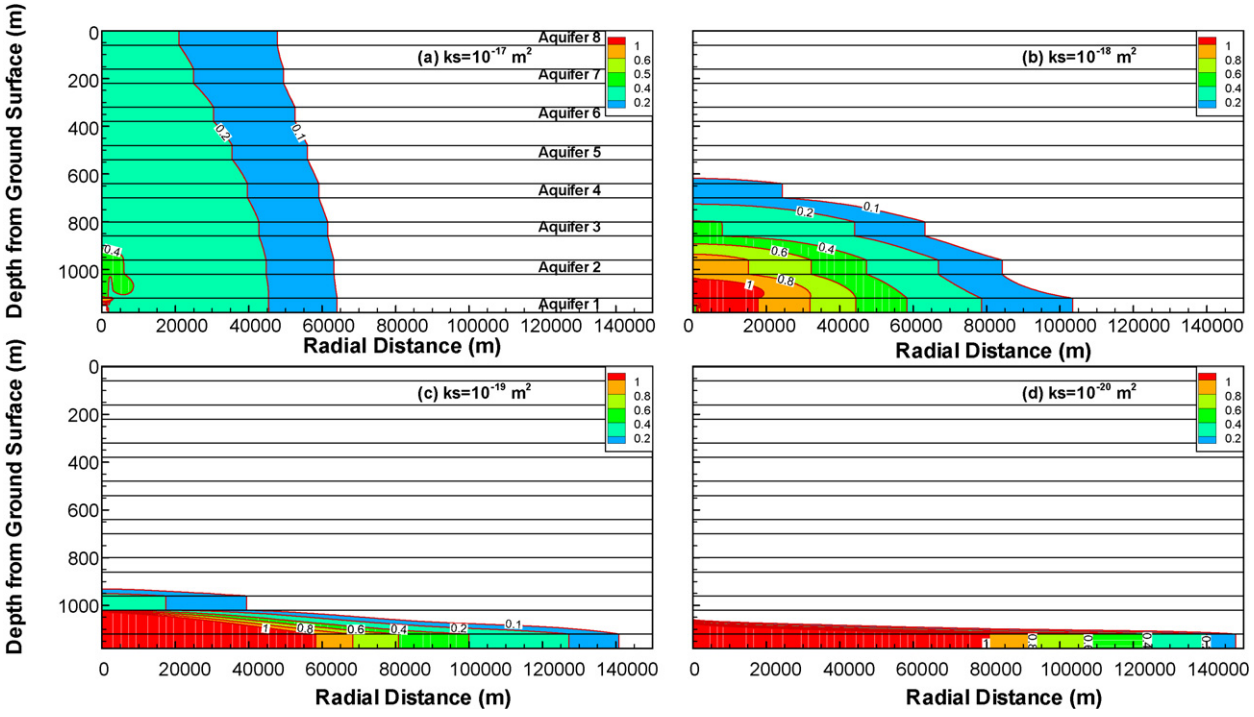

Fig. 6 – Contours of pressure buildup, given in bar (change in fluid pressure from the initial hydrostatic condition) 70 years after the end of CO_2 injection, for different values of seal permeability. A cutoff value of 0.1 bar is set for the contours. k_s means seal permeability.

contorted by the strongly exaggerated vertical-to-horizontal scale ratio, the pressure contours in Fig. 5 show the predominantly horizontal flow within the aquifers (vertical contours) versus the predominantly vertical flow within the seals (subhorizontal contours).

Fig. 6 shows the pressure buildup for the same four cases during the post-injection period, 70 years after injection ceases. Compared to Fig. 5, the pressure perturbations have relaxed significantly, with maximum pressure increases not much above 1 bar near the injection zone. However, as maximum pressure tends to return to an equilibrium state, the area of influence widens considerably. In the low-permeability case (10^{-20} m^2), a pressure increase of 0.1 bar extends now more than 140 km laterally within the storage formation, while vertical pressure changes above the deep saline aquifer are still insignificant. The high-permeability case (10^{-17} m^2), on the other hand, suggests that pressure perturbation can reach the uppermost aquifer, with maximum pressure increase of 0.2 bar and above, which corresponds to a change of about 2 m in the groundwater piezometric surface of the confined aquifer.

Fig. 7 shows the evolution of pressure change in three different stratigraphic units: (1) in the storage formation, (2) in Aquifer 5, and (3) in the top aquifer (Aquifer 8). Results are presented for all seal-permeability cases ranging from zero to 10^{-16} m^2 at different lateral distances (i.e., $R = 10$, 20, 50, and 100 km) from the injection zone. Notice that the pressure range displayed in the y-axis of the graphs varies. The transient pressure buildup in the storage formation (bottom row of plots in Fig. 7) is significantly affected by both radial location and seal permeability. Pressure buildup is larger close to the injection zone; also, the response time at the beginning and end of injection is shorter. Further away, the pressure response is weaker and occurs later. The maximum pressure is observed decades after injection stops when measured at 50 and 100 km radial extent. In fact, as Fig. 7(l) demonstrates, the pressure at a large distance from the injection zone is still increasing at 100 years, suggesting that it will take much longer for the hydrological system to reclaim a complete equilibrium state.

While the strong dependence of pressure buildup on radial location may be expected (in particular in a radial-symmetric setting), the significant impact of seal permeability is surprising. From the observed behavior, one may group all cases with seal permeability equal to or lower than 10^{-20} m^2 into an ''impermeable-seal'' category; these cases all feature similar pressure transients showing the strongest pressure perturbation in the storage formation. Relative to this, all other cases show moderate to drastic reduction in the maximum pressure – about 20% in the 10^{-19} m^2 case, about 50% in the 10^{-18} m^2 case, about 80% in the 10^{-17} m^2 case, and about 90% in the 10^{-16} m^2 case (based on the 20 km radial extent graph) – demonstrating the importance of interlayer brine flow.

The middle row of plots in Fig. 7 shows pressure evolution in Aquifer 5, which is the deepest aquifer of the freshwater zone extending from the ground surface to 540 m depth. Aquifer 5 is separated from the storage formation by four sealing layers. Over the 100 years of the simulation period, pressure impacts in this aquifer are observed only in the three cases with relatively high seal permeabilities (10^{-16}, 10^{-17}, and 10^{-18} m^2), the magnitude of pressure buildup depending on the radial location and the seal permeability. The maximum pressure increases – about 1.5, 0.6, and 0.05 bar, respectively at

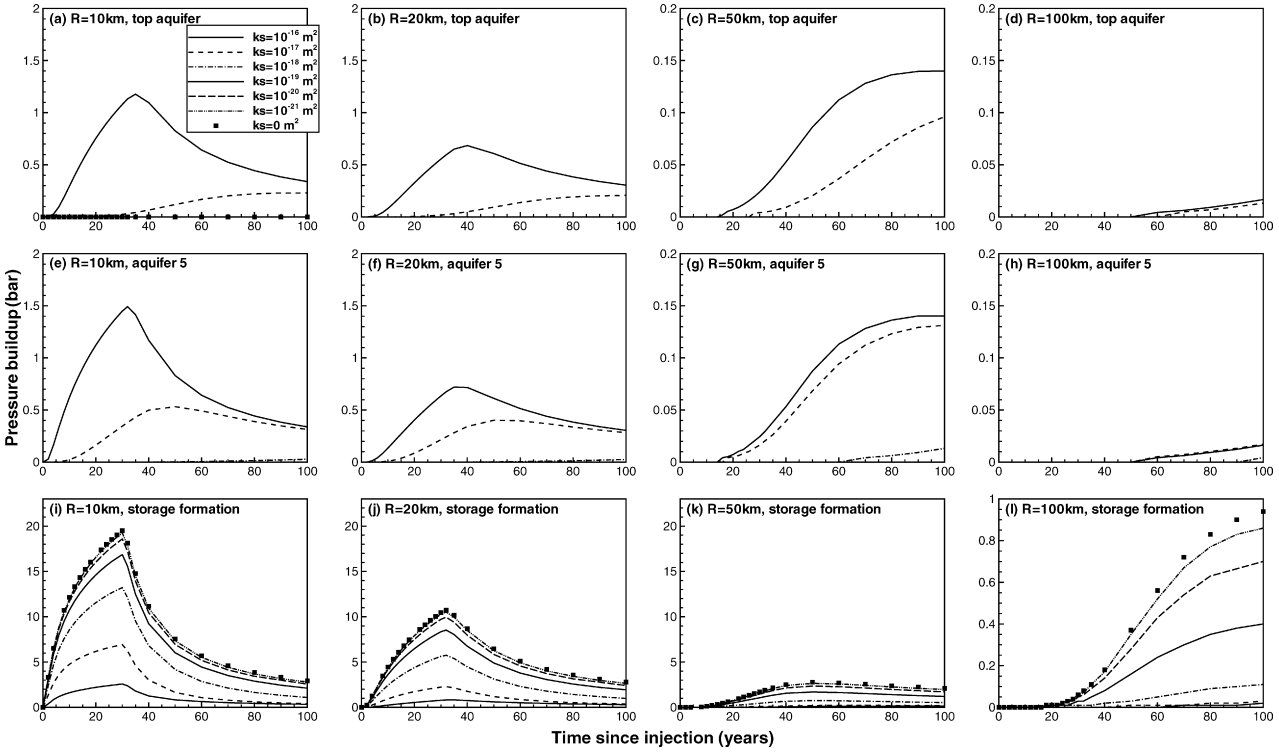

Fig. 7 – Sensitivity of pressure evolution to seal permeability. Pressure results are plotted at different radial locations and in different aquifers, starting with the deep storage formation (bottom row), Aquifer 5 (middle row), and the top aquifer (top row). k_s means seal permeability.

R = 10 km – are much smaller than those measured in the storage formation.

The pressure evolution in the uppermost aquifer is shown in the top row of Fig. 7, which is simulated as a confined unit in this study. Pressure increases are only observed for the two cases with highest seal permeability, with maximum pressure buildup of about 1.1 bar for the 10^{-16} m^2 case and about 0.2 bar for the 10^{-17} m^2 case (at a radial distance of 10 km from the injection zone). These values correspond to changes in the piezometric head of 11 and 2 m, respectively. The groundwater table changes to be expected in an unconfined aquifer can be estimated from the predicted pressure changes, equating the compressibility-related pore space increase in the confined system to the additional pore space occupied by water table rise. The storativity of the confined aquifer can be calculated as $S_s = b\phi\rho_w g(\beta_w + \beta_p) = 9.41 \times 10^{-5}$, where the aquifer thickness is b = 60 m, porosity is ϕ = 0.2, water density is $\rho_w = 1000\,\mathrm{kg/m^3}$, gravity acceleration is $g = 9.8\,\mathrm{m/s^2}$, and water and pore compressibility are $\beta_w = 3.5 \times 10^{-10}\,\mathrm{Pa^{-1}}$ and $\beta_p = 4.5 \times 10^{-10}\,\mathrm{Pa^{-1}}$, respectively. Multiplying storativity with predicted pressure increase and dividing by porosity gives the approximate water table rise in an unconfined aquifer, which ends up as 0.5 mm for the 1.1 bar pressure increase and 0.1 mm for the 0.2 bar pressure increase. These potential rises in the groundwater table are negligibly small.

3.3. *Characteristics of brine displacement*

We discuss here the possible implications that arise from the displacement and migration of native brine in response to CO_2 injection. Specifically, we evaluate the total volumetric brine flow in the lateral direction, at different radial cross-sections within the storage formation (Fig. 8), and the total volumetric interlayer brine flow in the vertical direction between different aquifers/aquitards (Fig. 9).

For reference, the volumetric brine flow is compared in Fig. 8 to the volumetric CO_2 injection rate, which is about 5300 m^3/day at storage conditions. Notice the modest changes in CO_2 injection rate, indicative of changes in pressure conditions (and related CO_2 density changes) during the injection period. (The plot shows the volumetric CO_2 injection rate for the specific pressure conditions obtained with a seal permeability of 10^{-16} m^2.) If there was pure piston-type flow in the storage formation, i.e., without compressibility effects and assuming impermeable seals, the volumetric rate of brine displacement at any radial location would be approximately equal to the volumetric rate of CO_2 injection. The results in Fig. 8 demonstrate, however, that both compressibility and brine leakage into nonideal seals are important in reducing the brine flow rates in the storage formation to much less than the CO_2 injection rates. Compressibility is the dominant factor in the 10^{-21} and 10^{-20} m^2 sensitivity cases, in which brine leakage out of the storage formation is not significant. Since the effect of compressibility increases with the volume affected by pressure changes, the volumetric rate of brine displacement depends strongly on radial location. For example, the maximum brine flow rate through the lateral cross-section at 10 km is about 4700 m^3/day, or about 90% of the volumetric CO_2 flow rate. The maximum brine flow rate reduces to about 600 m^3/day at 100 km, or about 10% of the volumetric CO_2 flow rate.

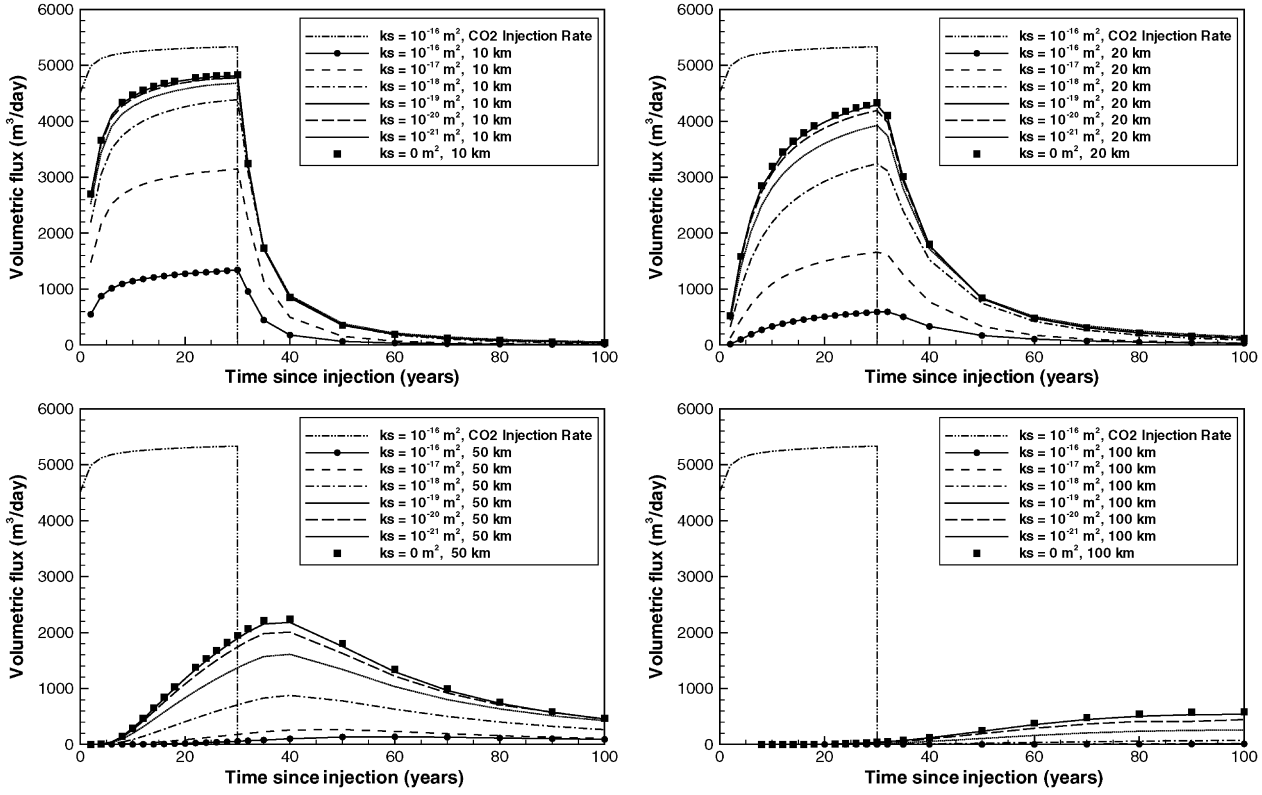

Fig. 8 – Evolution of total volumetric brine flux in the storage formation, for different seal permeabilities and radial locations. The brine flux is integrated over the entire cross-sectional (radial-symmetric) interface at a given location. The volumetric CO_2 injection rate is shown for reference. k_s means seal permeability.

Brine leakage out of the storage formation into overlying units causes additional attenuation within the storage formation. For the case of a seal permeability of 10^{-16} m^2, for example, the maximum brine flow rate within the storage formation reduces to about 1300 m^3/day at 10 km and is near zero at 100 km. It becomes clear from these results that the impact of vertical interlayer communication through the sealing units needs to be considered when estimating environmental issues related to pressure buildup and brine displacement within storage formations. Our example results suggest that vertical brine leakage becomes important when the seal permeability is higher than 10^{-19} m^2.

While the pressure pulse generated in the injection zone propagates far, and considerable amounts of native fluid are displaced within the storage formation, the actual brine flow velocities and the corresponding migration distance of a fluid particle are quite small. As a quick reference, we may calculate the maximum possible transport velocity assuming a pure piston-type displacement flow in the storage formation. Because the model domain is radial-symmetric, a uniform volumetric flux equal to the injection rate of CO_2 corresponds to velocity values decreasing with radial distance. The piston-type transport velocities can be easily calculated using $v = Q/2\pi Rb\phi$, where Q (=5300 m^3/day) is the volumetric injection rate at the storage condition. The calculated values are about 2.6 m per year at 10 km, 1.3 per year at 20 km, 0.5 m per year at 50 km, and 0.25 m per year at 100 km. To put these numbers into perspective, the regional Darcy velocity in the Alberta Basin is 0.01 to 0.1 m per year, which translates to a transport velocity of 0.1 to 1 m per year (assuming an effective porosity of 0.1) (Bachu et al., 1994). In other words, even the upper bounding limits provided by the piston-flow estimates are not excessively large compared to the natural groundwater velocities in deep basins.

Furthermore, without going into detail, the upper bound limits from a piston-type assumption are similar to the simulated lateral velocities only for small radii and small seal permeabilities. In all other cases, compressibility and/or brine leakage into upper strata reduce the actual transport velocities to a fraction of the piston-flow estimates. Furthermore, these velocities would decrease strongly after injection ceases and the system slowly returns to equilibrium. For reference, we may calculate upper-bound estimates for the lateral migration distance of brine using the piston-type transport velocity of 2.6 m per day at 10 km. The maximum migration distance would then be a few hundred meters over a 100-year period. This is rather insignificant and would suggest that environmental impacts related to updip displacement of saline or brackish water should be small, at least in a setting where radial-symmetric flow is a reasonable approximation.

Fig. 9 shows the evolution of the total volumetric interlayer brine/water flow rate in the vertical direction, integrated over the entire interface between aquifers and aquitards (from the injection zone to the lateral model boundary at R = 200 km). Results are provided (1) for the vertical flow out of the storage aquifer into the overlying aquitard, (2) for the vertical flow

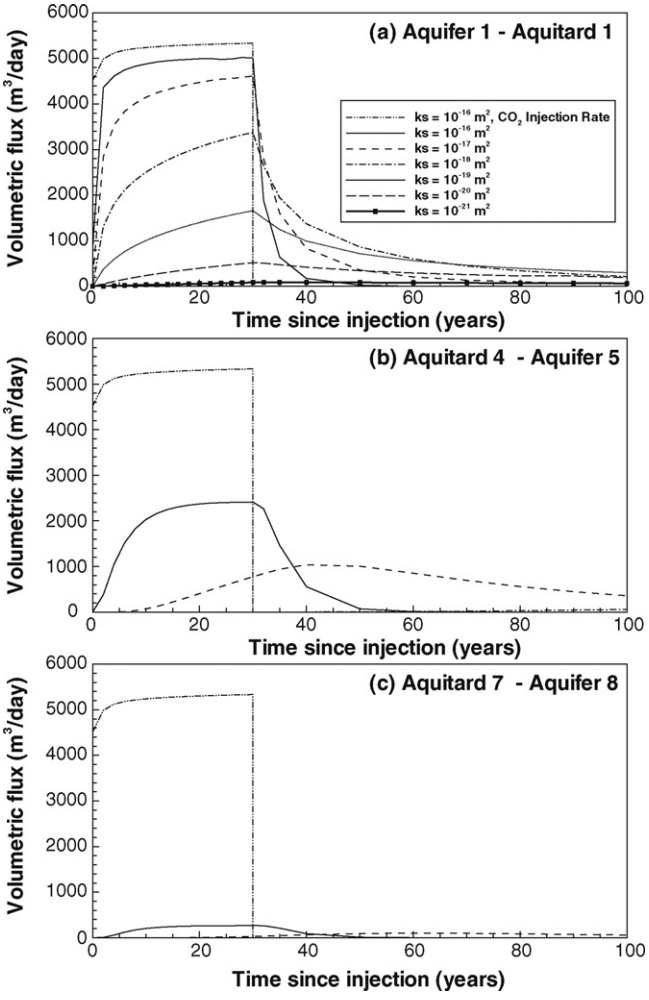

Fig. 9 – Evolution of total volumetric water flux across the entire interface between selected layers of the geologic system, for different seal permeabilities. Results are given for the interface between the storage formation and Aquitard 1, between Aquitard 4 and Aquifer 5, and between Aquitard 7 and Aquifer 8. The volumetric CO_2 injection rate is shown for reference. k_s means seal permeability.

from Aquitard 4 into Aquifer 5, and (3) for the vertical flow from Aquitard 7 into the uppermost aquifer (Aquifer 8) (see Fig. 2 for the schematic stratigraphy). In the case with the highest seal permeability of 10^{-16} m^2, vertical leakage of brine out of the storage formation is quite dominant (i.e., 94% of the fluid displaced by CO_2 leaves the storage formation and migrates upward). While the amount of water transferred between different layers decreases with increasing vertical distance from the storage formation, demonstrating the attenuation capacity of the overlying strata, the water flux into the top aquifer is still significant at about 5% of the CO_2 injection rate. However, these vertical fluxes decrease strongly with reducing seal permeability. For the case of a seal permeability of 10^{-18} m^2, significant vertical flux is only observed from the storage formation into the adjacent seal and from Aquitard 4 into Aquifer 5. Even smaller seal permeabilities (10^{-19} and 10^{-20} m^2) exhibit vertical brine leakage only from the storage formation into the adjacent seal; there is essentially no vertical water flux above the first sealing layer.

It is important to realize that the vertical flux of water between communicating strata does not correspond to a significant vertical displacement of deep brine into shallow units, because the vertical transport velocities are almost negligibly small. As a result, the initial vertical profile of salinity remains virtually unchanged during the simulation period. Fig. 10 displays the increases in salt mass fraction at 100 years compared to the initial condition in a vertical profile at a radius of 5 km, for the sensitivity case with a seal permeability of 10^{-17} m^2. Despite the relatively high seal permeability, the maximum increase in salt mass fraction is on the order of only 0.0003, corresponding to a relative salinity change of less than 0.2%. The changes in salinity occur predominantly in the deep aquitards, indicative of more saline water from underlying aquifers migrating into the seals.

Table 2 provides additional evidence for the insignificance of vertical displacement of brine, listing the vertical transport velocities at 30 years (1) in Aquitard 1, just above the storage formation, (2) in Aquitard 4, just below the deepest freshwater aquifer, and (3) in Aquitard 7, just below the top aquifer, for

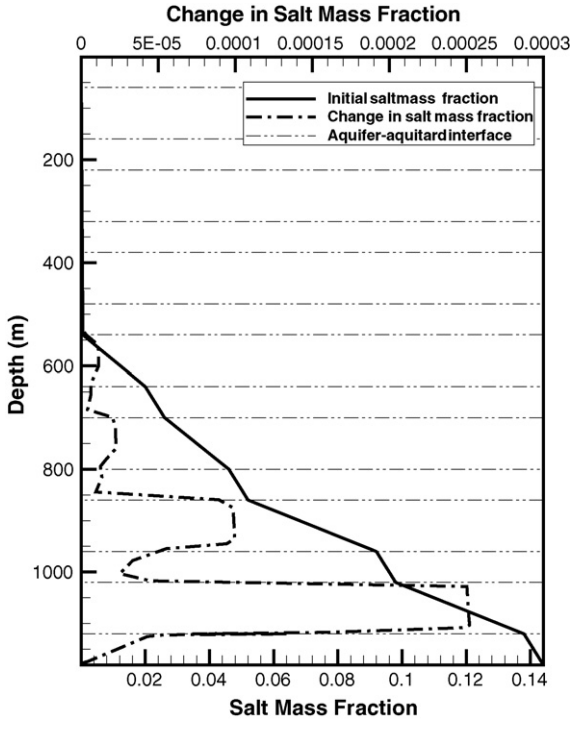

Fig. 10 – Vertical profile of salinity increases (given as salt mass fraction) at 100 years after the start of CO_2 injection compared to initial condition. Results are given at a radius of 5.0 km from the injection zone for the case with a seal permeability of 10^{-17} m^2.

different seal-permeability cases. These velocities at 30 years can provide upper-bound estimates of the vertical transport during the injection and post-injection period. For example, over a time period of 100 years, the maximum vertical transport distance in any sealing layer would be less than 1 m. (The relatively small velocity of brine transport through the sealing units results from the significantly large interface area available for vertical brine migration and the relatively low seal permeability, even though the volumetric flux is large.) This simplified analysis demonstrates that upward movement of saline water into shallow freshwater resources, via a sequence of aquifers and aquitards, is not a realistic environmental threat, unless high-permeability conduits, such as faults or abandoned boreholes, would provide direct hydraulic communication.

3.4. *Further sensitivities*

With sensitivity to seal permeability clearly established in the previous sections, we have conducted further sensitivity analysis to evaluate the impact of other parameters and properties on the large-scale lateral and vertical pressure perturbation and brine displacement. Important parameters and properties to consider would be the pore compressibility of the various strata, the thickness, permeability and porosity of the storage formation, the depth of storage formation and its distance to freshwater aquifers, the characteristics of the stratigraphic system, and the CO_2 injection rate and volume. For the given model setup, the CO_2 injection rate cannot be increased much further, because the observed injection pressure is already close to the assumed sustainable threshold (i.e., 150% of the hydrostatic pressure). An increase in CO_2 injection rate would have to be accommodated by optimized injection strategies (e.g., horizontal wells), or would require a more permeable and vertically extensive storage formation.

For brevity, we present here a few sensitivity cases addressing the role of pore compressibility. Using the base case with a seal permeability of 10^{-18} m^2 as a starting point, the following additional simulation runs were conducted: (1) the pore compressibility of all layers is considered to vary linearly with depth, starting with the values given in Table 1 for the deepest aquifer and aquitard, respectively, and assuming a one-order-of-magnitude increase over the entire vertical sequence, (2) the pore compressibility in all layers is increased by a factor of 10, and (3) the pore compressibility in all layers is reduced by a factor of 10.

Results are depicted in Fig. 11, showing vertical pressure profiles at radial extents of 10 and 50 km, for the different sensitivity cases, at the end of the injection period of 30 years and at 100 years after start of injection. A linear depth-dependence in pore compressibility has minor effects on the pressure results in comparison with the base case, mostly because the largest compressibility differences are in the uppermost layers where the pressure impact of CO_2 injection

Table 2 – Vertical upward pore velocity (in m per year) in three selected aquitards at 30 years and at radial location R = 10 km, as a function of seal permeability

Seal permeability	Aquitard 1 (above storage formation)		Aquitard 4 (below the deepest freshwater aquifer)		Aquitard 7 (below top freshwater aquifer)	
	Pore velocity (in m per year)	Distance in 100 years (m)	Pore velocity (in m per year)	Distance in 100 years (m)	Pore velocity (in m per year)	Distance in 100 years (m)
10^{-16} m^2	0.006	0.6	0.006	0.6	0.001	0.1
10^{-17} m^2	0.008	0.8	0.001	0.1	5×10^{-5}	0
10^{-18} m^2	0.003	0.3	4×10^{-7}	0	0	0
10^{-19} m^2	0.002	0.2	0	0	0	0
10^{-20} m^2	8×10^{-9}	0	0	0	0	0
10^{-21} m^2	0	0	0	0	0	0

In addition to pore velocity, this table also provides vertical travel distance, assuming that this pore velocity would be sustained over a 100-year time period.

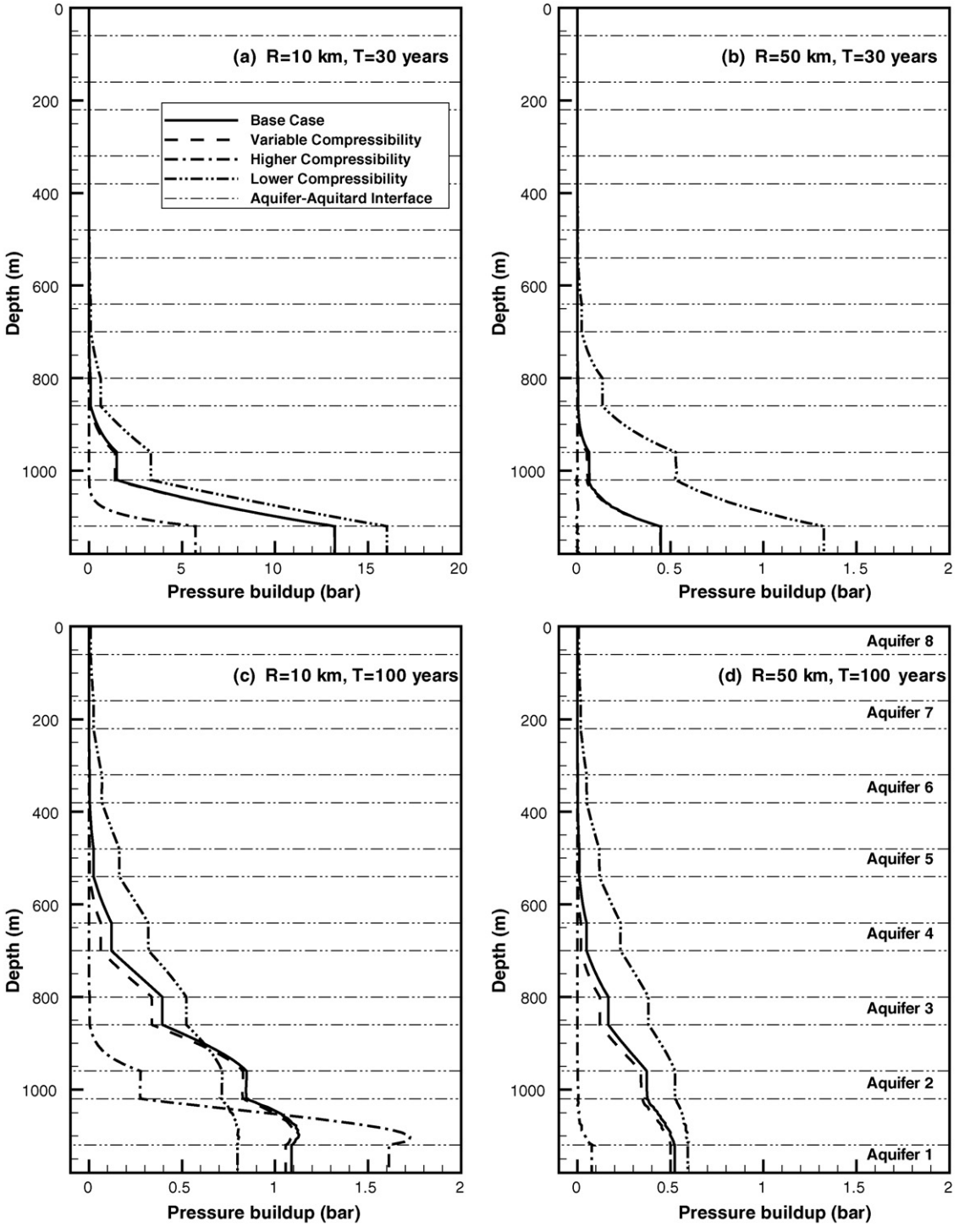

Fig. 11 – Vertical pressure profiles at 10 and 50 km radius for 30 and 100 years since start of CO_2 injection, for different compressibility sensitivity cases.

is very small. Stronger sensitivity is evident in the two other cases. An overall one-order-of magnitude reduction in pore compressibility causes a higher pressure buildup in the storage formation, as well as a larger region of influence, in both the lateral and the vertical direction. At 100 years, pressure changes propagate almost up to the top aquifer in this low-compressibility case. An opposite effect can be seen when compressibility in all layers is increased by a factor of 10. Here, the magnitude and spatial extent of pressure buildup is much smaller than in the base case. The exception is the pressure response in the storage formation and the overlying aquitard (Aquitard 1) during the post-injection period at 100 years. The pressure value at 10 km is the highest of all cases, caused by the increase in compressibility and the

resultant reduction in hydraulic diffusivity, defined by $k/\phi\rho_w\mu_w(\beta_w+\beta_p)$, where k is permeability and μ_w is water viscosity. The slower, diffusion-like equilibration process of near-field and far-field pressures for the higher pore compressibility case also depends on the system conditions at the start of the post-injection period.

4. Discussion

With respect to pressure changes *within* the storage formation, the region of influence in response to CO_2 injection can be extremely large. For the radial-symmetric domain evaluated in this study, considerable pressure buildup was observed at large distances of more than 100 km from the injection zone. Such pressure changes may cause problems if experienced in near-surface groundwater systems, a possible concern in a storage formation that extends updip to a shallow freshwater resource zone (Nicot, 2008). The extremely large area of influence observed with respect to pressure buildup may have important implications for the maximum CO_2 storage capacity at a given site, because such environmental impacts need to be avoided. Issues related to large-scale pressure buildup may also cause operational problems. For example, if more than one large CO_2 storage projects were intended in the same deep formation, the operational scheme and the location of the injection zones would have to be carefully planned to avoid unwanted feedback.

While the pressure pulse travels fast and far within the storage formation, the lateral brine flow velocities are quite small, not much larger than those of natural groundwater flows in deep basins. The migration distance of a particle dissolved in brine, indicative of the possible lateral displacement of saline water into freshwater resources, is only a few hundred meters or less for a time period of 100 years during and after injection. We caution that these results have been obtained for a radial-symmetric system, which is a reasonable approximation for a single-source injection site.

The characteristics of pressure buildup within the storage formation are strongly affected by the properties of the overlying multilayer aquitard/aquifer units. Seals suitable for long-term trapping of CO_2 but with relatively high permeability may allow for considerable brine leakage vertically out of the storage formation. As a result, the pressure buildup and lateral flow in the storage formation may be moderately to strongly reduced compared to a perfect seal with zero or close-to-zero permeability (i.e., less than 10^{-20} m^2). Note that if the storage formation was located above a sequence of layers with non-zero permeability, rather than situated on top of impermeable bedrock as assumed in this study, the pressure buildup within the storage formation and the overlying aquifers/aquitards would reduce further, depending on the permeability and thickness of the underlying aquifers and aquitards.

Our simulation results indicate that interlayer pressure propagation through a sequence of aquitards/aquifers is not very likely to affect shallow aquifers. Moderate pressure increases may occur in shallow freshwater aquifers only in cases with seal permeabilities on the order of 10^{-18} or more. Whether these perturbations could cause environmental problems depends on the specifics of the affected groundwater systems. For example, a pressure increase of less than a bar would be of lesser concern in a deep confined aquifer (such as Aquifer 5 in Fig. 2), but could cause negative effects in confined shallow groundwater resources (such as Aquifer 8 in Fig. 2) that communicate directly with surface water systems through localized leaky pathways (e.g., faults and boreholes). Without such leaky pathways, the estimated changes in the groundwater table of unconfined aquifers are on the order of less than a millimeter, certainly too small to change the groundwater flow regime and affect the rates of discharge into lakes or streams (Bergman and Winter, 1995). Furthermore, many groundwater systems have been severely overused as a source for municipal or agricultural water supply; the resulting aquifer drawdowns dwarf the above projected increases in the piezometric surface or water table caused by CO_2 injection and storage.

Vertical interlayer migration of saline water through the sequence of layers towards shallow aquifers is also not a realistic concern, as indicated by the close-to-zero vertical transport velocities. These conclusions, however, would change if deep and shallow units would communicate via local high-permeability conduits such as faults and abandoned boreholes. This relevant topic is outside the scope of this study.

Note that the pressure buildup and brine migration in both lateral and vertical directions discussed above are for the case of a single CO_2 storage site in a large sedimentary basin with an area of 125,000 km^2 (R = 200 km). In our simulation scenario, the storage efficiency, calculated as the volume of stored CO_2 divided by the total pore space in the storage formation, is rather small at 4.0×10^{-5} (Zhou et al., 2008). It is possible that multiple injection sites are needed in such a large sedimentary basin in order to accommodate the CO_2 volumes stemming from various industrial-scale emitters. For example, if a storage efficiency of 2% was to be achieved (IPCC, 2005; USDOE, 2007), one would need about 500 injection sites with the same injection rate and period as those used in this study. This would correspond to a average spacing of only about 16 km between different injection sites, suggesting that interference between individual sites would be likely. Superposition of the solutions obtained in this study for a single injection site may be used to approximate the overall system response to multiple injection sites. Site-specific basin-scale modeling with realistic multiple injection/storage sites will be conducted in our future investigations.

5. Summary and conclusions

Through numerical modeling of idealized subsurface formations with a single injection site, we have evaluated the possible impact of industrial-scale CO_2 injection on regional multilayered groundwater systems. For the conditions evaluated in this study, considerable pressure buildup in the storage formation is predicted more than 100 km away from the injection zone, while the lateral brine transport velocity and migration distance are less significant. Large-scale pressure changes appear to be of more concern to groundwater resources than changes in water quality, due to (for example) the lateral migration of saline waters.

Seal permeability has a significant impact on pressure buildup and brine displacement behavior within the storage formation. Seals with relatively high permeability but still suitable for long-term trapping of CO_2 allow for considerable brine leakage out of the formation vertically upward and/or downward. As a result, the pressure buildup in the storage formation can be strongly reduced compared to a perfect seal with zero or close-to-zero permeability. In such cases, one needs to ensure that vertical pressure propagation and brine migration have no negative impact on freshwater aquifers. Modeling results, however, suggest that brine migration through a sequence of layers into shallow groundwater bodies is extremely unlikely. Pressure perturbation of shallow units may occur only when the permeability of sealing layers is comparably high.

Our results clearly demonstrate the importance of evaluating the large-scale hydrologic perturbations generated by CO_2 storage. Any site assessment should consider the constraints imposed by pressure perturbation, ideally in modeling studies that fully account for the multilayer characteristics of the storage site. While some key properties of multilayered groundwater systems have been varied in a sensitivity study, which has enabled us to draw general conclusions, certain model simplifications, specifications, and parameter choices may be inadequate at given storage sites. Thus, the systematic simulations conducted here should lead into site-specific modeling of CO_2 storage candidate sites, representing the local hydrogeological conditions.

Acknowledgments

The authors wish to thank Larry Myer at Lawrence Berkeley National Laboratory (LBNL) for his careful internal review of the manuscript. Thanks are also due to two anonymous reviewers for their constructive suggestions for improving the quality of the manuscript. This work was funded by the Assistant Secretary for Fossil Energy, Office of Sequestration, Hydrogen, and Clean Coal Fuels, National Energy Technology Laboratory, of the U.S. Department of Energy, and by Lawrence Berkeley National Laboratory under Contract No. DE-AC02-05CH11231.

REFERENCES

Bachu, S., Gunter, W.D., Perkins, E.H., 1994. Aquifer disposal of CO_2: hydrodynamic and mineral trapping. Energy Convers. Manage. 35 (4), 269–279.

Bergman, M., Winter, E.M., 1995. Disposal of carbon dioxide in aquifers in the U.S. Energy Convers. Manage. 36, 523–526.

Chadwick, A., Arts, R., Bernstone, C., May, F., Thibeau, S., Zweigel, P., 2007. Best Practice for the Storage of CO_2 in Saline Aquifers: Observations and Guidelines from the SACS and CO2STORE Projects.

Domenico, P.A., Schwartz, F.W., 1998. Physical and Chemical Hydrogeology, 2nd ed. John Wiley & Sons, Inc., New York.

Fjaer, E., Holt, R.M., Horsrud, P., Raaen, A.M., 1991. Petroleum Related Rock Mechanics. Elsevier, Amsterdam.

Gale, J., 2004. Geological storage of CO_2: what do we know, where are the gaps, and what more needs to be done? Energy 29 (9–10), 1329–1338.

Gunter, W.D., Bachu, S., Law, D.H.-S., Marwaha, V., Drysdale, D.L., McDonald, D.E., McCann, T.J., 1996. Technical and economic feasibility of CO_2 disposal in aquifers within the Alberta sedimentary basin, Canada. Energy Convers. Manage. 37 (6–8), 1135–1142.

Harris, J.M., 2006. Seismic Monitoring of CO_2 Sequestration. GCEP Technical Report. Stanford University, Palo Alto, CA, USA.

Hart, D.J., 2000. Laboratory Measurements of Poroelastic Constants and Flow Parameters and Some Associated Phenomena. Ph.D. Thesis. University of Wisconsin-Madison, Madison, WI, USA.

Hart, D.J., Bradbury, K.R., Feinstein, D.T., 2006. The vertical hydraulic conductivity of an aquitard at two spatial scales. Ground Water 44 (2), 201–211.

Hepple, R.P., Benson, S.M., 2005. Geologic storage of carbon dioxide as a climate change mitigation strategy: performance requirements and the implications of surface seepage. Environ. Geol. 47, 576–585.

Holloway, S., 1996. An overview of the Joule II Project: the underground disposal of carbon dioxide. Energy Convers. Manage. 37 (6–8), 1149–1154.

Holloway, S., 2005. Underground sequestration of carbon dioxide—a viable greenhouse gas mitigation option. Energy 30, 2318–2333.

Hovorka, S.D., Doughty, C., Knox, P.R., Green, C.T., Pruess, K., Benson, S.M., 2001. Evaluation of brine-bearing sands of the Frio formation, upper Texas gulf coast for geological sequestration of CO_2. In: First National Conference on Carbon Sequestration, National Energy Technology Laboratory, Pittsburgh, PA, USA, 14–17 May, p. 2001.

IPCC (Intergovernmental Panel on Climate Change), 2005. IPCC Special Report on Carbon Dioxide Capture and Storage. Cambridge University Press, New York.

Neuzil, C.E., 1994. How permeable are clays and shales? Water Resour. Res. 30 (2), 145–150.

Nicot, J.-P., 2008. Evaluation of large-scale CO_2 storage on fresh-water sections of aquifers: an example from the Texas Gulf Coast Basin. Int. J. Greenhouse Gas Control 2, 582–593.

Pruess, K., 2005. ECO2N: A TOUGH2 Fluid Property Module f or Mixtures of Water, NaCl, and CO_2. Report LBNL-57952. Lawrence Berkeley National Laboratory, Berkeley, CA, USA.

Pruess, K., Oldenburg, C.M., Moridis, G., 1999. TOUGH2 User's Guide, Version 2.0. Report LBNL-43134. Lawrence Berkeley National Laboratory, Berkeley, CA, USA.

USDOE (U.S. Department of Energy), 2007. Methodology for development of carbon sequestration capacity estimates, Appendix A in Carbon Sequestration Atlas of the United States and Canada, National Energy Technology Laboratory, Pittsburgh, PA, USA.

USEPA (U.S. Environmental Protection Agency), 1994. Determination of Maximum Injection Pressure for Class I Wells, United States Environmental Protection Agency Region 5—Underground Injection Control Section Regional Guidance #7. EPA, Washington DC, USA.

USGS (U.S. Geological Survey), 1999. Land Subsidence in the United States. U.S. Geological Survey Circular 1182, Reston, Virginia, USA.

Van der Meer, L.G.H., 1992. Investigations regarding the storage of carbon dioxide in aquifers in the Netherlands. Energy Convers. Manage. 33 (5–8), 611–618.

Van Genuchten, M.T., 1980. A closed form equation for predicting the hydraulic conductivity of unsaturated soils. Soil Sci. Soc. Am. J. 44, 892–898.

Zhou, Q., Birkholzer, J.T., Tsang, C.-F., Rutqvist, J., 2008. A method for quick assessment of CO_2 storage capacity in closed and semi-closed saline formations. Int. J. Greenhouse Gas Control 2, 626–639.